DIRECT NUMERICAL SIMULATIONS OF THE TURBULENT CONVECTION AND THERMAL RADIATION IN A RAYLEIGH-BÉNARD CELL

Tomasz Czarnota
Institute for Aerodynamics and Flow Technology
German Aerospace Center (DLR)
Bunsenstrasse 10, 37073 Göttingen, Germany
Tomasz.Czarnota@dlr.de

Claus Wagner
Institute for Aerodynamics and Flow Technology
German Aerospace Center (DLR)
Bunsenstrasse 10, 37073 Göttingen, Germany
Claus.Wagner@dlr.de

ABSTRACT

We perform direct numerical simulations (DNS) of turbulent Rayleigh-Bénard convection coupled with surface-to-surface radiation in a rectangular enclosure filled with air to investigate whether this interaction influences the heat transfer, temperature distribution and the flow structures. To do so, horizontal solid plates with finite conductivity are employed for the considered Rayleigh-Bénard cell. Such boundary conditions allow local variations of the temperature at the hot and cold interfaces due to their interaction with the fluid and surface radiation. In order to investigate the maximum effect of those boundary conditions, both interfaces are treated as a blackbody ($\varepsilon = 1$) and the cell is filled with a radiatively non-participating fluid (Prandtl number Pr=0.7). The effects of radiation for highly conducting plates are shown and compared to the case where radiation is neglected.

It is found that due to highly conducting plates the mean temperature at the interfaces changes only 0.04% from the one of the infinite conductive plates. Furthermore, we observe that due to surface-to-surface radiation coupled with highly conducting plates, the mean temperature at the interfaces changes 0.1% at the interfaces and 0.2% in the bulk. It is shown that the temperature at the hot interface tends to decrease due to the radiative heat loss while the temperature at the cold interface slightly increases. Apart from that, we observe small changes in the temperature distribution at the interfaces due to surface-to-surface radiation. We notice that the highest temperatures at the top interface appear in the middle and the values steadily decrease towards the edges.

Additionally, we observe a small drop of the convective Nusselt number and little variations of the temperature distribution at the interfaces. Finally, it is shown that all mentioned variations caused by heat radiation between interfaces are too small to visibly change the large scale flow structures when highly conducting plates are employed. It is also shown that in the non-radiation case of poorly conducting plates the heat transfer and the temperature variations at the interfaces are influenced significantly.

INTRODUCTION

Turbulent Rayleigh-Bénard convection (RBC) is one of the classical problems of fluid dynamics. Despite the great effort made in the past to understand the complex physical mechanisms in this type of flow, there are still many open questions which must be answered. Besides that, the effect of thermal radiation on turbulent RBC is also of interest since so far not many conducted investigations address this problem. The reason might be that modeling thermal radiation is computationally expensive. One possibility to decrease this effort in numerical simulations of heat radiation and turbulent convection is to assume that the radiation does not depend on the wavelength and to approximate the directional nature by diffuse emission. Nevertheless, the intensity of irradiation still depends on the geometrical features and thermal properties of radiatively interacting surfaces. Hence, simulating heat radiation in a Direct Numerical Simulation of turbulent Rayleigh-Bénard convection slows down the computation by a factor of 20.

The effect of conductive horizontal plates was investigated in many experimental and numerical studies (see Brown et al. 2005, Verzicco and Sreenivasan 2008, Johnston and Doering 2009). Fixed temperature boundary conditions correspond to an infinite thermal conductivity of the plates while an imposed heat flux models poorly conducting plates. Their studies indicated that the heat transfer is suppressed for $Ra > 10^9$ in simulations with plates of finite conductivity whereas for lower Ra the two boundaries lead to a similar flow. Apart from that, Balaji and Venkateshan (1993, 1994) and Akiyama and Chong (1997) performed numerical

simulations of a square cavity filled with air with gray surfaces heated and cooled from the sides. They noticed that the convective heat transfer is suppressed due to surface radiation and the radiative heat transfer at the heated and cooled walls increases greatly with the emissivity of the walls. They also noted that the surface radiation alters significantly the temperature distribution inside the cavity and the flow patterns. However, in their simulations the flow was steady, laminar and two-dimensional. Nevertheless, the results of Verzicco and Sreenivasan (2008) or Johnston and Doering (2009) as well as those of Balaji and Venkateshan (1993, 1994) or Akiyama and Chong (1997) refer to a cell with infinitely thin plates while the finite thickness of the plates is modelled in our computations. Such boundary conditions allow changes of the temperature at the hot and cold interfaces due to turbulent convection and surface radiation.

In this study, the effects of radiation are shown and compared to the case when radiation is neglected. We observe a similar drop of convective Nusselt number as Akiyama and Chong (1997) and Ridouane et al. (2004). However, in our configuration this change of convective Nu due to exchange of radiation between interfaces is too small to visibly change the large scale flow structures. It is also shown that poorly conducting plates significantly influence the heat transfer and the temperature variations at the interfaces. Hence, future simulations of RBC coupled with surface radiation might reveal greater changes in the heat transfer and large scale flow structures when less conductive materials of the solid plates are employed.

NUMERICAL PROCEDURE

Direct numerical simulations are conducted in the rectangular domain with aspect ratio $\Gamma = \hat{W}/\hat{H} = 1$, where $\hat{H}$ is the height and $\hat{W}$ the width of the enclosed fluid. No-slip and impermeability conditions are applied to all solid walls, so that velocity components $\hat{u}_i|_{wall} = 0$. The outer sides of the top and bottom solid plates are isothermal with non-dimensional temperatures $T_{top} = -0.5$ and $T_{bot} = +0.5$, respectively. Adiabatic lateral walls are realized in the spanwise direction and in the longitudinal direction of length $\hat{L} = 5\hat{H}$ by means of a zero temperature gradient perpendicular to the wall, i.e. $\partial\hat{T}/\partial\hat{x} = 0$; $\partial\hat{T}/\partial\hat{y} = 0$. Additionally, the irradiation which reaches a surface on the side walls is directly reflected to the origin surface, hence only the temperature at the interfaces can change due to radiation. Fig. 1 illustrates the geometry and boundary conditions used in this study. The dimensionless thickness of the heating and cooling plates equals $h_s = h_h = h_c = 0.065$. In the simulation where radiation is taken into account the solid plates are made out of aluminium. However, to simplify the problem and to investigate the maximal influence of surface-to-surface radiation, both interfaces are treated as a blackbody ($\varepsilon = 1$). Furthermore, we assume that the working fluid is a radiatively non-participating medium of Prandtl number Pr = 0.7. The considered governing equations are the incompressible Navier-Stokes equations derived under the assumption of the Boussinesq approximation. Their non-dimensionalisation is carried out using $x_i = \hat{x}_i/\hat{H}$, $u_i = \hat{u}_i/(\hat{\alpha}\hat{g}\Delta\hat{T}\hat{H})^{1/2}$, $T = (\hat{T} - \hat{T}_0)/\Delta\hat{T}$, $p = \hat{p}/(\hat{\rho}\hat{\alpha}\hat{g}\hat{H}\Delta\hat{T})$ and $t = \hat{t}(\hat{\alpha}\hat{g}\hat{H}\Delta\hat{T})^{1/2}/\hat{H}$, where $\hat{\alpha}$ is the thermal expansion coefficient and $\hat{\rho}$ is the density. $\hat{g}$ represents the gravitational acceleration which acts in vertical z-direction. $\Delta\hat{T}$ denotes the temperature difference between the outer sides of the heating and cooling plates and $\hat{H}$ is the height of the fluid layer. We denote dimensional quantities with $\hat{}$ and dimensionless without. Finally, the dimensionless form of the governing equations is given by equation (1) - (3).

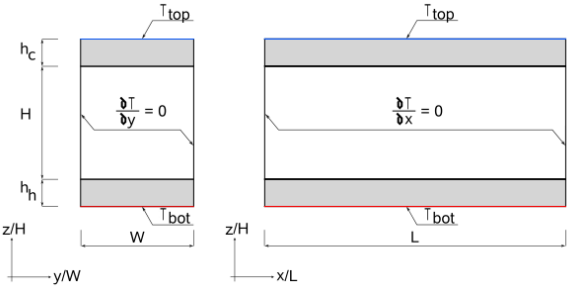

Figure 1. Geometry of the convection cell with temperature boundary conditions.

$$\frac{\partial u_j}{\partial x_j} = 0 \tag{1}$$

$$\frac{\partial u_i}{\partial t} + u_j\frac{\partial u_i}{\partial x_j} + \frac{\partial p}{\partial x_i} = \nu\frac{\partial^2 u_i}{\partial x_j^2} + T\delta_{3i} \tag{2}$$

$$\frac{\partial T}{\partial t} + u_j\frac{\partial T}{\partial x_j} = \kappa_f\frac{\partial^2 T}{\partial x_j^2} \tag{3}$$

Here, $u_i (i = x, y, z)$ are the velocity components in i direction, T and p represent the temperature and pressure, respectively and δ_{ij} is a Kronecker symbol. The non-dimensional kinematic viscosity and thermal diffusivity are defined by (4) and (5), respectively.

$$\nu = \left(\frac{Pr}{Ra}\right)^{1/2} \tag{4}$$

$$\kappa_f = \frac{1}{(RaPr)^{1/2}} \tag{5}$$

The dimensionless control parameters, Prandtl and Rayleigh numbers, are defined by (6) and (7), respectively and their values are presented in table (1).

$$Pr = \frac{\hat{\nu}}{\hat{\kappa}_f} \tag{6}$$

$$Ra = \frac{\hat{\alpha}\hat{g}\hat{H}^3\Delta\hat{T}}{\hat{\nu}\hat{\kappa}_f} \tag{7}$$

The boundary conditions at the interfaces impose the same heat flux on both sides as described by equation (8) - (9) and the solution of this equation determines the temperature at the interfaces. In simulations which do not account for

thermal radiation, the radiative heat fluxes represented by q_e and q_{ir} are neglected.

$$bottom\ interface: \quad q_{c,s}+q_{ir} = q_{c,f}+q_e \tag{8}$$

$$top\ interface: \quad q_{c,f}+q_{ir} = q_{c,s}+q_e \tag{9}$$

$$q_{c,s} = -\frac{\hat{k}_s}{\hat{k}_f}\frac{\partial T}{\partial x}|_{s.side} \tag{10}$$

$$q_{c,f} = -\frac{\partial T}{\partial x}|_{f.side} \tag{11}$$

$$q_e = Nr(T_i+\theta)^4 \tag{12}$$

$$q_{ir} = Nr\sum_{S_j}(T_j+\theta)^4 F_{ij} \tag{13}$$

Here, $q_{c,s}$ and $q_{c,f}$ represent conductive heat fluxes from the solid and fluid side of the interface, respectively; $\hat{k}_s/\hat{k}_f$ denotes the ratio of thermal conductivity for solid and fluid. Including equation (12) and (13) in the boundary conditions for radiation implies, that additional control parameters like conduction-radiation number Nr and the temperature ratio θ defined by (14) and (15), respectively have to be fixed. Table (1) summarizes the value of the control parameters used in the considered simulations.

$$Nr = \frac{\hat{\sigma}\Delta\hat{T}^3\hat{H}}{\hat{k}_f} \tag{14}$$

$$\theta = \frac{\hat{T}_0}{\Delta\hat{T}} = \frac{0.5(\hat{T}_{bot}+\hat{T}_{top})}{\hat{T}_{bot}-\hat{T}_{top}} \tag{15}$$

In equation (13) the summation over the surface element S_j is done for all the elements in the boundary with which the element i can interact radiatively. The view factors are determined by a function of the geometry and they are calculated from equation (16) as proposed by Incropera et al. (2006).

$$F_{ij} = A_j\frac{cos\phi_i cos\phi_j}{\Pi R_{ij}^2} \tag{16}$$

Here, A_j is an area of a surface j and the polar angles ϕ_i and ϕ_j are formed between the line connecting the centers of the surface i and j and the surface normals n_i and n_j, respectively. R_{ij} is a distance between surface i and j. In the present study we simulate Rayleigh-Bénard convection for two different thermal boundary conditions at the horizontal plates. One is called 'aluminium-fluid case' and the other one 'plexiglas-fluid case' assuming that the solid plates are made out of aluminium and plexiglas, respectively. Considering aluminium the thermal diffusivity $\hat{\kappa}_s$ equals $8.418\times10^{-5}m^2/s$, while for plexiglas $\hat{\kappa}_s = 7.49\times10^{-8}m^2/s$ and for air $\hat{\kappa}_f = 2.216\times10^{-5}m^2/s$. The term 'radiation case' is used for the simulation concerning aluminium plates. Additionally, the results obtained for the 'solid-fluid cases' are compared with those where the heating and cooling plates are isothermal and infinitely thin: h_h and $h_c \to 0$ ('fluid case').

Table 1. Values of dimensionless control parameters and dimensional properties used in considered simulations.

Ra [-]	Pr [-]	Nr [-]	θ [-]	$\hat{T}_0$ [K]	$\Delta\hat{T}$ [K]	$\hat{H}$ [m]
$6.3x10^7$	0.7	0.0006	39.2	332	8.46	0.5

Applying the boundary conditions described in equation (8) - (9) is only possible by approximating the temperature at the interfaces. Thus, in order to choose the best approximation of $(T+\theta)^4$ two different methods were tested. Deriving the temperature at the interfaces around heating/cooling plate using Taylor Series Expansion gave approximation errors of order 10^{-3}. By using the Newton-Raphson's method it was possible to decrease the approximation error to 10^{-11} in most cases after 3 iterations.

The convective heat flux, represented by the Nusselt number Nu_c, is calculated for both radiation and non-radiation cases with equation (17).

$$Nu_c = \frac{\langle\hat{u}_z\hat{T}\rangle_{t,S_z} - \hat{\kappa}_f\langle\frac{\partial\hat{T}}{\partial\hat{x}_z}\rangle_{t,S_z}}{\hat{\kappa}_f\Delta\hat{T}/\hat{H}} = \sqrt{RaPr}\langle u_z T\rangle_{t,S_z} - \langle\frac{\partial T}{\partial x_z}\rangle_{t,S_z} \tag{17}$$

where $\langle\cdot\rangle_{t,S_z}$ denotes averaging in time and in vertical z direction. Additionally, at the interfaces contributions of both convection and radiation should be taken into consideration in the expression of Nu. Thus, the total Nusselt number at the interfaces for each i-th surface is calculated as $Nu = Nu_c + Nu_r$, where Nu_r reads

$$Nu_r = \frac{\hat{\sigma}\hat{T}_i^4 - \sum_{S_j}\hat{\sigma}\hat{T}_j^4 F_{ij}}{\hat{\kappa}_f\Delta\hat{T}/\hat{H}} = Nr(T_i+\theta)^4 - \sum_{S_j}Nr(T_j+\theta)^4 F_{ij} \tag{18}$$

The method used for DNS is based on the volume balance procedure by Schumann et al. (1979) and the second order accurate explicit Euler-Leapfrog time discretisation scheme. Spatial derivaties and cell face velocities are approximated by piecewise integrated fourth-order accurate polynomials, where the velocity components are stored on staggered grids as described in more detail in Shishkina and Wagner (2007). In order to sufficiently resolve the boundary layers the minimum number of nodes in the thermal boundary layer is estimated for all considered cases with the criterion by Shishkina et al. (2010) which provides the needed grid points to sufficiently resolve a Prandtl-Blasius type boundary layer. The grid spacing needed to resolve all relevant turbulent scales in the core region is estimated according to Grötzbach (1983) and in every direction is smaller than the Kolmogorov length. Finally, to satisfy the above requirements performing our simulations for the Rayleigh number $Ra = 6.3x10^7$, we use 10 grid points to resolve the thermal boundary layer and $256x256x576$ grid points in vertical, spanwise and longitudinal direction, respectively.

RESULTS

Temperature analysis

The mean temperature at the interfaces together with it's spatial deviation is shown in table 2. It is found that for highly

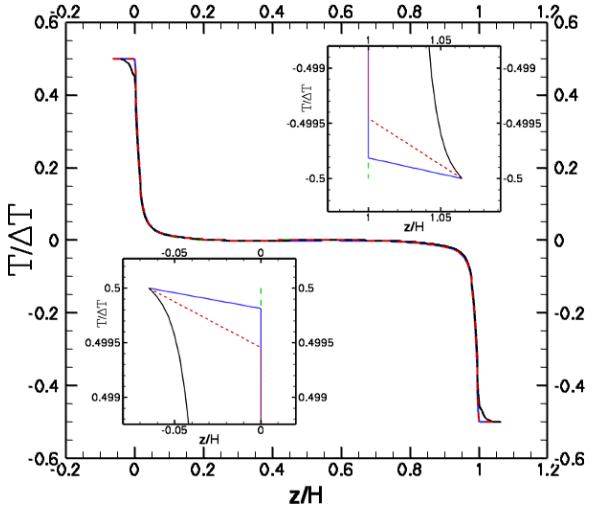

Figure 2. Time and area averaged temperature profiles for $Ra = 6.3x10^7$, close-up views for bottom (left fig.) and top (right fig.) solid plates; fluid case (– –), aluminium-fluid case (—), plexiglas-fluid case (—), radiation case (- -).

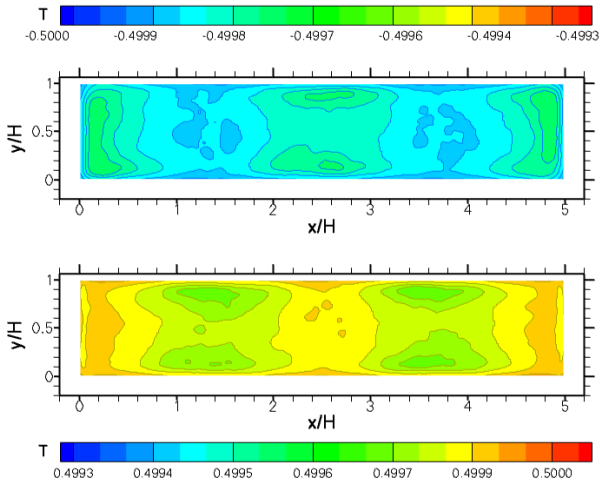

Figure 3. Time averaged temperature distribution at the top (top fig.) and bottom (bottom fig.) interface; aluminium-fluid case, $Ra = 6.3x10^7$.

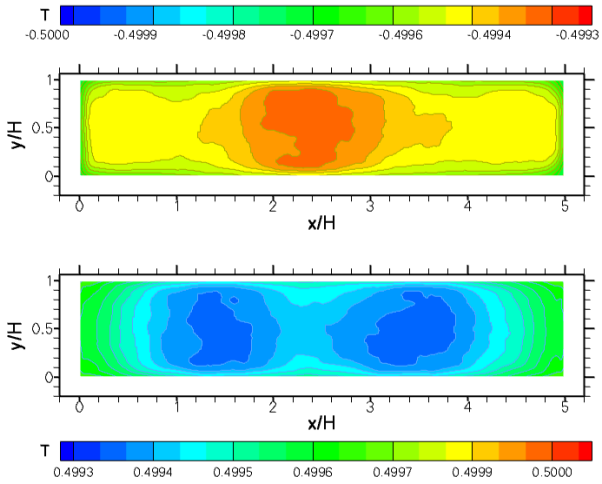

Figure 4. Time averaged temperature distribution at the top (top fig.) and bottom (bottom fig.) interface; radiation case, $Ra = 6.3x10^7$.

conducting plates (here represented by the aluminium-fluid case) the deviation of the temperature at the interfaces is very small. This denotes nearly a homogenous temperature distribution and thus, a small contribution of turbulent convection on the temperature distribution at the interfaces. Additionally, figure 2 reveals that for the aluminium-fluid case the mean temperature at the interfaces differs only 0.04% compared to the one of the infinite conductive plates (fluid case). This implies that the contribution of thermal conductivity to a change of the mean temperature at the interfaces is very high.

Analysing the mean temperature for the radiation case (see figure 2), we observe that the temperature changes 0.1% at the interfaces and 0.2% in the bulk in comparison to the infinitely thin plates with isothermal conditions (fluid case). In details, the temperature at the bottom interface decreases and the temperature at the top interface increases. Those temperature changes are related with the net radiation which is directed from hotter to colder interface. Thus, the top interface gains the heat which is lost by the bottom interface. Despite the fact, that the changes of temperatures for the radiation case are small, it is noteworthy that the temperature drop at the bottom interface due to radiation is 50% higher than the one obtained for the highly conducting aluminium plates.

Additionally, comparing the radiation case to the aluminium-fluid case, small differences in the temperature distribution at the interfaces are found. Because of a small

Table 2. Time and volume averaged convective Nusselt number (Nu_c). In addition, time and area averaged temperature with spatial deviations; convective, radiative and total Nusselt number ($Nu_c, Nu_r, Nu_{bot/top}$) at the bottom/top interfaces.

		bottom (hot) interface				top (cold) interface			
case	Nu_c	T	Nu_c	Nu_r	Nu_{bot}	T	Nu_c	Nu_r	Nu_{top}
aluminium-fluid	27.29	$0.4998 \pm 4.3x10^{-5}$	27.30	0.0	27.30	$-0.4998 \pm 4.5x10^{-5}$	27.20	0.0	27.2
radiation	27.12	$0.4995 \pm 1.1x10^{-4}$	27.20	52.13	79.33	$-0.4995 \pm 6.5x10^{-5}$	27.08	52.13	79.21
plexiglas-fluid	23.63	$0.4472 \pm 1.2x10^{-2}$	23.68	0.0	23.68	$-0.4476 \pm 1.4x10^{-2}$	23.60	0.0	23.6

spatial temperature deviations at the interfaces we plot the results in figure 3 and 4 in a close-up view with scales ranging from -0.5 to -0.4993 and 0.4993 to 0.5 for the top and bottom interfaces, respectively. For the radiation case we notice that the highest temperatures at the top interface appear in the middle and the values steadily decrease towards the edges while there are four symmetric hot spots for the aluminium-fluid case.

Finally, we conclude that surface-to-surface radiation influence the temperature distribution at the interfaces and the mean profiles, however these variations from the isothermal conditions (fluid case) are small.

Analysing the plexiglas-fluid case we observe a similar effect to the one detected for the radiation case. Figure 2 shows vertical temperature distribution in the bulk and in the vicinity of the plates in a close-up view. It is visible that due to poorly conducting plates the temperature at the bottom interface decreases and the temperature at the top interface increases about 10% in comparison to the isothermal case (fluid case). For poorly conducting plates rising and descending convective plumes can easily modify the temperature at the interfaces and lead to non-uniform temperature distribution.

The spatial temperature deviations of the temperature at the interfaces are shown in table 2. The highest values are obtained for poorly conducting plates what denotes the most non-uniform temperature distribution at the interfaces compared to the other cases. From the above results, we conclude that poorly conducting plates decrease the contribution of the thermal conductivity to the changes of the mean temperature at the interfaces in favour of turbulent convection and possibly thermal radiation. Hence, future simulations of RBC coupled with surface radiation might reveal even larger changes of the temperature values at the interfaces when less conductive materials of the solid plates are employed.

Analysis of Nusselt numbers and temperature gradients

The results summarized in table 2 reveal that the total heat transfer at the interfaces (Nu_{bot}/Nu_{top}) is nearly 3 times higher in the radiation case than in the case where radiation is neglected (aluminium-fluid case). The radiative heat flux emitted from the bottom interface does not interact with the medium but is absorbed directly by a colder, top interface. That causes the higher heat flux at the top interface and finally higher temperature gradients inside the aluminium plate, see figure 5. The evaluation of the radiative heat transfer at the hot interface was also investigated by Ridouane et al. (2004, 2006). According to their studies the value of Nu_r is higher when the emissivity of the surfaces is higher and in addition Nu_r increases quickly with Ra as ilustrated in a graph for Ra ranging from 10^3 to $2.3x10^6$. In our study we present the results for $Ra = 6.3x10^7$ which are in a good agreement with the extrapolated values of Ridouane et al. (2004, 2006).

Further, the time and volume averaged Nusselt number Nu_c, shown in table 2, is lower for the radiation case compared to the aluminium-fluid case. Finally, surface-to-surface radiation reduces the convective effect by about 0.6%. Similar conclusions were reported by Akiyama and Chong (1997) and later by Ridouane et al. (2004) who studied the problem of a square enclosure with gray surfaces for different emissivities.

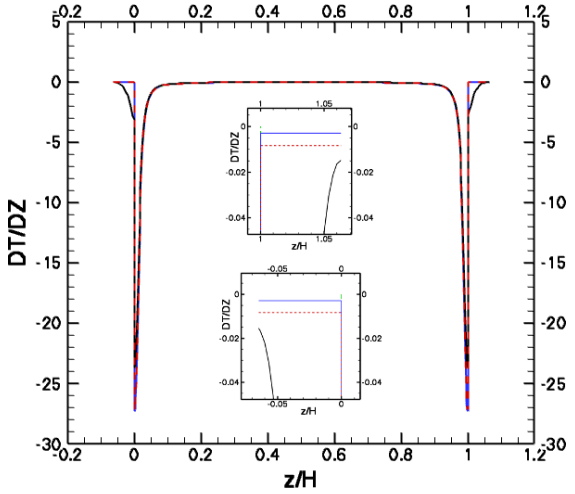

Figure 5. Time and area averaged temperature gradient profiles for $Ra = 6.3x10^7$, close-up views for bottom (lower inset) and top (upper inset) solid plates; fluid case (– –), aluminium-fluid case (—), plexiglas-fluid case (—), radiation case (- -).

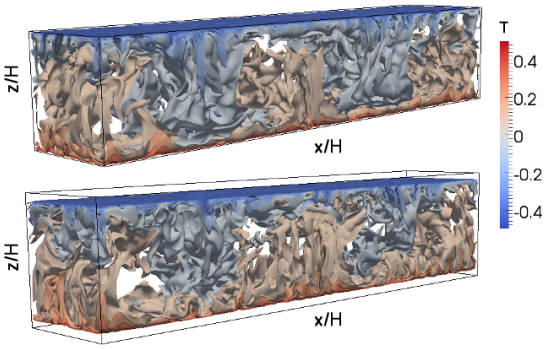

Figure 6. Instantaneous temperature distribution for the fluid case (upper figure), the radiation case (lower figure); $Ra = 6.3x10^7$.

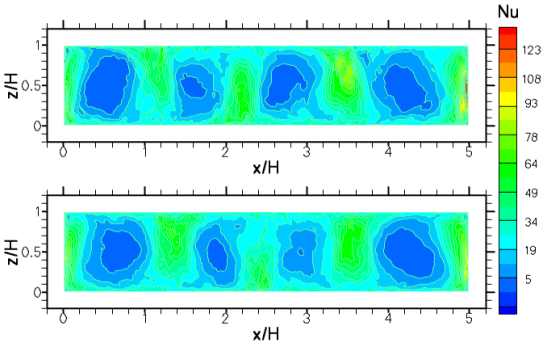

Figure 7. Distribution of the local, time averaged convective Nusselt number plotted at y/Z=0.5 for the fluid case (upper figure), the radiation case (lower figure). $Ra = 6.3x10^7$.

Analysis of the large scale flow structures

Instantaneous flow fields obtained for isothermal conditions (fluid case) and the radiation case are presented in fig-

ure 6. In both cases the large scale plumes forming the large scale circulation disintegrate into smaller plumes. The shape of these large scale structures and the temperature on the heating and cooling boundaries are similar for the fluid case and the radiation case.

Additionally, figure 7 shows a two dimensional distribution of the time averaged convective Nusselt number (Nu_c) to demonstrate the fingerprints of the generated large scale flow structures in detail. Two smaller structures in the middle of the cell and two bigger ones close to the vertical walls are present for the radiation case and for the fluid case. However, due to small variations in the convective Nusselt number (Nu_c) and similar temperature values at the interfaces, the differences between corresponding flow structures are hardly visible.

CONCLUSIONS

Many numerical studies of Rayleigh-Bénard convection performed in the past use fixed temperature or fixed flux boundary conditions for infinitely thin plates. In the present study we assume fixed temperature boundary conditions at the outer side of the solid plates with finite thickness. Using such boundary conditions allows to implement surface-to-surface radiation and analyse the changes of the temperature distribution and the heat transfer on the heating and cooling boundaries (solid-fluid interfaces). In order to investigate the maximum effect of the boundary conditions, both interfaces are treated as a blackbody ($\varepsilon = 1$) and the cell is filled with a radiatively non-participating fluid.

Analysing the results of the conducted direct numerical simulations for $Ra = 6.3x10^7$, it is found that due to surface-to-surface radiation coupled with highly conducting plates, the temperature changes 0.1% at the interfaces and 0.2% in the bulk in comparison to the infinitely thin plates with isothermal conditions. Additionally, the temperature at the hot interface decreases due to radiative heat loss and the temperature at the cold interface increases. Apart from that, we observe small changes in the temperature distribution at the interfaces due to surface-to-surface radiation. We notice that the highest temperatures at the top interface appear in the middle and the values steadily decrease towards the edges.

Finally, we conclude that surface-to-surface radiation influences the temperature distribution at the interfaces and the mean temperature profiles, however these variations from the isothermal conditions (fluid case) are small.

We observe a small reduction of convective effect due to radiation. The similar drop of the convective Nusselt number was also reported by Akiyama and Chong (1997) and Ridouane et al. (2004) in their 2D simulations of a square cavity. Due to the small variations in the convective Nusselt number (Nu_c) and similar temperature at the interfaces for the radiation case and the isothermal case, the differences in large scale flow structures are hardly visible.

The analysis of the results for poorly conducting plates (plexiglas-fluid case) reveals that these boundary conditions significantly influence the heat transfer and the temperature distribution at the interfaces. The temperature at the bottom interface decreases about 10% and at the top interface increases. This effect is similar to the one observed for the radiation case but the influence of the temperature is much higher for the plexiglas-fluid case than for the radiation case. Finally, we suppose that future simulations of RBC coupled with surface radiation might reveal greater changes in the heat transfer and some changes in the flow structures when less conductive materials of the solid plates are employed.

Acknowledgments

The authors would like to thank Sebastian Wagner for fruitful discussions and suggestions.

REFERENCES

Akiyama, M. and Chong, Q. P., 1997, "Numerical analysis of natural convection with surface radiation in a square enclosure", Numerical Heat Transfer, Part A: Applications, 32: 4, pp. 419-433.

Balaji, C. and Venkateshan, S. P., 1993, "Interaction of surface radiation with free convection in a square cavity", Int. J. Heat Fluid Flow, Vol. 14, no. 3, pp. 260-267.

Balaji, C. and Venkateshan, S. P., 1994, "Correlations for free convection and surface radiation in a square cavity", Int. J. Heat Fluid Flow, Vol. 15, no. 3, pp. 249-251.

Brown, E., Nikolaenko, A., Funfschilling, D. and Ahlers, G., 2005, "Heat transport in turbulent Rayleigh-Bénard convection: Effect of finite top- and bottom-plate conductivity", Phys. Fluids, Vol. 17, 075108.

Grötzbach, G., 1983, "Spatial resolution requirements for direct numerical simulation of Rayleigh-Bénard convection", J. Comp. Phys., Vol. 49, pp. 241-264.

Incropera, F. P., DeWitt, D. P., Bergman, T. L., Lavine, A. S., 2006, "Fundamentals of Heat and Mass Transfer", 6th Edition.

Johnston, H. and Doering, C.R., 2009, "Comparison of Thermal Convection between Conditions of Constant Temperature and Constant Flux", PRL 102, 064501.

Ridouane, E. H., Hasnaoui M., Amahmid A. and Raji A., 2004, "Interaction between natural convection and radiation in a square cavity heated from below", Numerical Heat Transfer, Part A:Applications, 45: 289-311.

Ridouane, E. H., Hasnaoui M. and Campo A., 2006, "Effects of surface radiation on natural convection in a Rayleigh-Bénard square enclosure: steady and unsteady conditions", Heat and Mass Transfer, Vol. 42, Issue 3, pp. 214-225.

Schumann, U., Grötzbach, G. and Kleiser, L., 1979, "Direct numerical simulations of turbulence, In Prediction Methods for Turbulent Flows number", VKI-lecture series 1979 2. Von Kármán Institute for Fluid Dynamics.

Shishkina, O. and Wagner, C., 2007, "Boundary and interior layers in turbulent thermal convection in cylindrical containers", Int. J. Sci. Comp. Math., Vol. 1(2/3/4), pp. 360-373.

Shishkina, O., Stevens, R.J.A.M., Grossmann, S. and Lohse, D., 2010, "Boundary layer structure in turbulent thermal convection and its consequences for the required numerical resolution", New J. Phys., Vol. 12, 075022.

Verzicco, R. and Sreenivasan, K.R., 2008, "A comparison of turbulent thermal convection between conditions of constant temperature and constant heat flux", J. Fluid Mech., Vol. 595, pp. 203-219.